FREQUENCY DOMAIN TECHNIQUE FOR FAULT DIAGNOSIS IN ANALOG CIRCUITS-SOFTWARE AND HARDWARE IMPLEMENTATION

[1]V.PRASANNAMOORTHY [2]N. DEVARAJAN

[1]Asst Prof., Department of Electrical Engineering, GCT, Coimbatore – 641 013, India

[2]Assoc. Prof., Department of Electrical Engineering, GCT, Coimbatore – 641 013, India

ABSTRACT

In this paper, we present a fault diagnosis system for analog circuit testing based on the Simulation Before Test (SBT) approach. The circuit under test is subjected to a frequency response analysis, from which parameters are extracted such that they give unique values for every configuration of the circuit. This uniqueness makes them ideally suitable for utilization as signatures that may be used to characterize the state of the circuit. Software implementation has been done using MATLAB and SIMULINK, whereas, for the hardware implementation of the system, we have chosen the NI ELVIS platform. In both cases, signatures have been extracted from the frequency response of the circuit (Sallen-Key band pass filter). As most signature values obtained are unique, successful classification of faults is made feasible.

Keywords: *Circuit Under Test (CUT), Sallen-Key Band Pass Filter, Bode Plot, Peak Gain*

1. INTRODUCTION

An analog circuit is said to have a fault if the value of an element (component) or a measured output parameter (circuit characteristic) deviates from its designated value. Fault testing is performed with the objective of detection, location, or diagnosis. Fault detection simply identifies the presence of a fault in a circuit; fault location specifies the site where the circuit is faulty; fault diagnosis tells the exact value of the deviations from the nominal values. Fault location is used for repairing faulty parts at a later time, while fault diagnosis is needed for adjustment or tuning. Several researches [1]-[3] have addressed the issue of fault diagnosis of analog electronic circuits at the system board and chip level.

Fault diagnosis in analog electronic circuits is more complicated than digital circuits due to poor fault models component tolerances and nonlinear effects; diverse design styles and a multitude of response parameters make analog electronic circuit testing difficult and expensive. Testing the entire set of specifications for a Circuit under test (CUT) would provide complete confidence in the tested part. However, the time and cost overheads of such a procedure are high. Therefore, in practice, manufacturers test only a few specifications over a limited input space. The drawback is that such compromise can lessen the quality of circuits manufactured. Testing and diagnosis of electronic devices are fundamental topics in the development and maintenance of safe and reliable complex systems. In both cases, the attention is focused on the detection of faults affecting a system safety and performance.

Two major issues make the analysis particularly difficult: the complex nature of the fault mechanism, namely the physical/ chemical process leading to a failure, and the unknown values for the actual component parameters (which differ from the nominal values). Parameter deviations depend on the intrinsic nature of the production process of the component and on-the-field deviations such as those related to aging or thermal effects. Such situations which do not change the circuit topology are commonly defined as “soft” or parametric faults and may lead to unpredictable incorrect operations depending on their impact on the circuit performance.

Thus, before testing begins, we need to quantify the test effort and evaluate various test options to minimize cost and maximize confidence. This need motivates research in structured fault based approaches similar to those employed in digital circuits. In such approaches, fault models capture

the effect of physical defects on circuit behavior, fault simulation evaluates the detection capabilities of a test set on a set of faults(and measures fault coverage), and test generation derives minimal test set to detect those faults.

In a complete fault diagnosis procedure, fault detection and isolation must be carried out together; the effectiveness of the procedure depends on fault detection and isolation performance as well as the complexity of the test phase. This combination is often referred to as FDI [4], [5] (fault detection and isolation) in literature. There are two different approaches [6] are generally adopted to obtain an automatic diagnosis for an analog electronic circuit. They are Simulation After Test (SAT) and Simulation Before Test (SBT).

The simulation-after-test [6]-[8] approach involves the computation of various circuit parameters from the operational circuit and fault identification is carried out using these parameters, assuming that each measurement is independent of the other. Fault isolation is done by estimating the circuit parameters from the measured circuit outputs. The identification of the circuit parameters is based on the assumption that enough information is available in the measurements and that measurements are mutually independent. This method is avoided due to the increase in process time with increase in the size of the circuit, in addition to several drawbacks associated with nonlinear or local minima issues. The SBT approach [9]-[12] is based on the comparison of the circuit responses associated with predefined test stimuli with those induced by different fault conditions. A subsequent classification must be considered to solve the fault detection and isolation problems.

There are numerous techniques that may be applied for signature extraction from circuits such as using time domain analysis [13], [14] and other approaches [15]-[20]. In this paper, we propose a fault diagnosis technique that follows the SBT approach, involving the estimation of parameter values from the frequency response of the CUT which can then be used as signatures for the classification of faults.

2. DIAGNOSIS METHODOLOGY

The proposed methodology for fault diagnosis can be explained as a series of four distinct steps. They are as below:

1. The transfer function of the circuit under test is derived assuming nominal values for all circuit components. For our analysis, we have taken up the Sallen-Key band pass filter circuit as the circuit under test. As this circuit has already been used previously in other fault diagnosis studies and has been found to fairly tolerant to component variations, we found it to be a suitable choice.
2. The frequency response of the circuit is simulated in MATLAB. The fault-free condition is first checked and then, in a similar way, component values are made to deviate away their nominal values and the frequency response is recorded. This way, the signature parameters, namely the peak of the gain curve and the frequency at which this peak occurs, can be tabulated for every condition of the circuit.
3. The practical analysis is done with the help of NI ELVIS (NI Educational Laboratory Virtual Instrumentation Suite). The frequency response is again measured for all the circuit configurations and the parameter values are noted.

Using steps 3 and 4, fault dictionaries can be constructed for various deviations of component values, the data being organized in a systematic fashion.

3. CIRCUIT UNDER TEST

We have taken up the Sallen-Key band pass filter circuit to illustrate this approach. The Sallen-Key band pass filter, shown in Fig. 1, is a second order active filter, which is greatly appreciated for its simplicity of design.

Its transfer function is obtained as

$$G(s) = \frac{sA_0 G_1 C_1}{s^2 C_1 C_2 + s(G_2 C_1 + G_3 C_2 + G_1 C_1[1 - A_0]) + G_3(G_1 + G_2)}$$

where

$A_0 = 1 + (R_B/R_A)$, $G_1 = (1/R_1)$, $G_2 = (1/R_2)$, $G_3 = (1/R_3)$

The voltage divider in the negative feedback loop controls the gain. The "inner gain" G provided by the operational amplifier is given by

$$G = 1 + \frac{R_B}{R_A}$$

while the amplifier gain at the peak frequency is given by

$$A = \frac{G}{3 - G}$$

The value of G must be kept below 3 dB or else the filter will oscillate. The filter is usually optimized by selecting $R_2 = 2R_1$ and $C_1 = C_2$. Keeping these restraints and the availability of components in mind, we chose R_1=R_f=10 kΩ, R_2=22 kΩ, R_a=R_b=3.3 kΩ and C_1=C_2=0.1 μF.

The filter section shown in Fig. 1 can also be cascaded to form second order filter stages, resulting in larger order filters. The op-amp provides buffering between filter stages, so that each stage can be designed independently. This circuit is suitable for filters which have complex conjugate poles. When implementing a particular transfer function, a designer will typically find all the poles, and group them into real poles and complex conjugate pairs. Each of the complex conjugate pole pairs are then implemented with a Sallen-Key filter, and the circuits are cascaded together to form the complete filter.

4. SIGNATURE EXTRACTION

Since the two frequency domains specifications, namely the peak gain and the frequency at which this peak occurs, show distinct variations in reaction to certain changes in the component values in the CUT, they can be used as fault signatures with great efficacy as a direct reflection of the present condition of the system. There are essentially three phases in the process of building a fault dictionary [21], [22]. The first phase consists of choosing a suitable stimulus signal that can be used to simulate the circuit operation for all the anticipated faults and storage of the corresponding responses. The second phase involves selection of one or more points in the circuit where responses can be conveniently recorded. The final phase of the process is the matching of responses obtained from the CUT with those available in the fault dictionary.

The fault dictionary of a given circuit is prepared in such a manner to serve as a complete database of the responses expected from faults which have been experienced in the past or those which can be simulated. Sets of values unique to each faulty state of the circuit may be taken up as the signatures that characterize the respective states. The frequency response of the CUT is simulated for each fault in the dictionary and the resulting frequency domain response parameters are noted.

4.1 Theoretical Estimation of Parameters

In order to obtain the frequency response of the Sallen-Key band pass filter in theory, we chose to model the circuit in MATLAB [24] with the help of its transfer function. This was done using the *bode* function available in the Control System Toolbox of MATLAB. The frequency response of the circuit for the fault free condition obtained using the *bode* function is as shown in Fig. 2.

It may be noted from the figure that the maximum value that the gain of the filter reaches is 6.84 dB at a frequency of 154.45 Hz (970.44 rad/sec). These values may be tabulated as signatures that characterize the fault free state of the CUT. Now, for successful isolation of faulty configurations from this fault free configuration, it is essential that any deviation in component values gives rise to an altogether different pair of values for the parameters considered. For example, consider the configuration in which the value of the resistor R_a is raised by 50% beyond its nominal value .i.e. a change in resistance from 3.3 kΩ to 5.1 kΩ. For this configuration, there is a significant change in the peak value of the gain curve from that of the fault free state. To be more specific, the peak of the gain curve for the R_a+50% condition occurs at 151.75 Hz (953.47 rad/sec) and has a value of 2.31 dB. Thus, whenever there is a deviation of a component value from its nominal level, there is a corresponding variation seen in the peak gain and the frequency at which this peak occurs. This is the basic tenet on which our diagnosis methodology is based.

The two required frequency domain response parameter are noted for all the response curves. These, being characteristic to a particular configuration, are used as the fault signatures. The fault dictionaries for few single, double, triple and other multiple faults are presented in the tables I, II, III and IV respectively. The fault free condition is given the ID F61

TABLE I

FAULT DICTIONARY FOR SINGLE FAULTS

Fault ID	Faulty Components	Peak Gain (dB)	Frequency at Peak Gain (Hz)
F1	$R_1\uparrow$	6.65	146.78
F2	$R_1\downarrow$	6.12	199.53
F3	$R_2\uparrow$	10.19	135.94
F8	$R_b\downarrow$	-0.32	171.13
F9	$R_f\uparrow$	3.90	146.78
F10	$R_f\downarrow$	17.00	232.63
F11	$C_1\uparrow$	4.60	135.94
F12	$C_1\downarrow$	8.94	215.44
F13	$C_2\uparrow$	8.37	135.94
F14	$C_2\downarrow$	3.39	232.63

TABLE III

FAULT DICTIONARY FOR DOUBLE FAULTS

Fault ID	Faulty Components	Peak Gain (dB)	Frequency at Peak Gain (Hz)
F15	$R_1,R_2\uparrow$	13.70	115.38
F16	$R_1,R_2\downarrow$	2.44	273.75
F23	$R_a,R_f\uparrow$	0.94	138.46
F24	$R_a,R_f\downarrow$	2.44	167.11
F25	$R_a,C_1\uparrow$	0.87	123.82
F26	$R_a,C_1\downarrow$	15.80	214.85
F27	$R_a,C_2\uparrow$	3.42	123.82
F28	$R_a,C_2\downarrow$	25.80	213.27
F29	$R_f,C_1\uparrow$	2.68	113.16
F30	$R_f,C_1\downarrow$	17.00	267.38

TABLE IIIII

FAULT DICTIONARY FOR TRIPLE FAULTS

Fault ID	Faulty Components	Peak Gain (dB)	Frequency at Peak Gain (Hz)
F35	$R_1,R_2,C_1\uparrow$	9.95	92.63
F36	$R_1,R_2,C_1\downarrow$	4.05	386.74
F37	$R_a,R_b,C_2\uparrow$	8.43	124.14
F42	$R_1,R_a,C_1\downarrow$	23.00	259.42
F43	$R_2,R_a,C_1\uparrow$	3.42	101.22
F44	$R_2,R_a,C_1\downarrow$	20.50	310.35
F47	$R_2,R_f,C_1\uparrow$	5.26	92.30
F48	$R_2,R_f,C_1\downarrow$	11.40	391.52

TABLE IV

FAULT DICTIONARY FOR OTHER MULTIPLE FAULTS

Fault ID	Faulty Components	Peak Gain (dB)	Frequency at Peak Gain (Hz)
F49	$R_1,R_2,R_a,R_f\uparrow$	2.31	101.22
F50	$R_1,R_2,R_a,R_f\downarrow$	25.00	311.94
F51	$R_1,R_2,R_a,C_1\uparrow$	2.93	0.00
F55	$R_2,R_b,C_1,C_2\uparrow$	32.50	82.44
F56	$R_2,R_b,C_1,C_2\downarrow$	-4.86	450.40
F57	$R_b,R_f,C_1,C_2\uparrow$	9.24	92.31
F58	$R_b,R_f,C_1,C_2\downarrow$	3.22	845.11
F61	Fault Free	6.84	154.45

A general rule of thumb is that once the fault signatures have been collected and organized into a fault dictionary, the data must be optimized by eliminating signatures that bring about masking of faults whose signatures match. In the above tables, there arise two pairs of parameters possessing identical values. These give rise to two ambiguity sets, A_1 and A_2, each consisting of two faulty configurations which has been shown in table V.

TABLE V

AMBIGUITY SETS

Set	Fault ID	Faulty Components	Peak Gain (dB)	Frequency at Peak Gain (Hz)
A_1	F13	$C_2\uparrow$	8.43	124.14
	F37	$R_a,R_b,C_2\uparrow$		
A_2	F14	$C_2\downarrow$	3.33	214.86
	F38	$R_a,R_b,C_2\downarrow$		

Both F13 and F37 achieve a peak gain of 8.43 dB at a frequency of 124.14 Hz. Due to this redundancy in behavior, it is not possible to differentiate between the two configurations. Similarly, F14 and F38 form another ambiguity set. The rest of the data is found to be free of redundancies, hence making it feasible to identify each faulty configuration on the basis of variations in two parameters alone.

4.2 Practical Estimation of Parameters

For practical estimation of the peak gain and the frequency at which it occurs, we chose to implement the circuit on the National Instruments Educational Laboratory Virtual Instrumentation Suite (NI ELVIS). The experiment set is represented in Fig.3. The Sallen-Key band pass filter circuit was setup on the prototyping board, with nominal values of components initially, following which, the component values were varied by 50% above or below their nominal levels. Once the circuit is setup, the frequency for the circuit can be determined by launching the Bode Analyzer through the NI ELVIS Instrument Launcher. The bode plot for the fault free condition is as shown in Fig. 4.

It may be noted from the figure that the maximum value that the gain of the filter reaches is 6.33 dB at a frequency of 158.49 Hz. These values may be tabulated as signatures for the fault free state. Again, any deviation in component values must necessarily produce deviations in the parameters considered. For the sake of comparison with the theoretical results, consider the configuration in which the value of the resistor R_a is raised by 50% beyond its nominal value .i.e. a change in resistance from 3.3 kΩ to 5.1 kΩ. For this configuration, as with the theoretical results, there is a significant change in the peak value of the gain curve from that of the fault free state. To be more specific, the peak of the gain curve for the R_a+50% condition occurs at 171.13 Hz and has a value of 2.03 dB. Also, as seen with the results obtained in MATLAB, there is a drop in the peak value of the gain curve in comparison to the fault free condition. This is confirmation that the behavior of the actual circuit on the prototyping board is in complete agreement with the theoretical model. However, one must note that unlike the theoretical results, one cannot expect to get the exact same values for parameters in the practical case. The parameter values vary with every trial taken, the variations being such that they are sufficiently distinct from each other to enable fault isolation without ambiguities.

The fault dictionaries for single, double, triple and other multiple faults, taken at one trial, are presented in the tables VI, VII, VIII and IX respectively. The fault free condition is given the ID F61.

TABLE VI

FAULT DICTIONARY FOR SINGLE FAULTS

Fault ID	Faulty Components	Peak Gain (dB)	Frequency at Peak Gain (Hz)
F1	$R_1\uparrow$	6.65	146.78
F2	$R_1\downarrow$	6.12	199.53
F3	$R_2\uparrow$	10.19	135.94
F8	$R_b\downarrow$	-0.32	171.13
F9	$R_f\uparrow$	3.90	146.78
F10	$R_f\downarrow$	17.00	232.63
F11	$C_1\uparrow$	4.60	135.94
F12	$C_1\downarrow$	8.94	215.44
F13	$C_2\uparrow$	8.37	135.94
F14	$C_2\downarrow$	3.39	232.63

TABLE VII

FAULT DICTIONARY FOR DOUBLE FAULTS

Fault ID	Faulty Components	Peak Gain (dB)	Frequency at Peak Gain (Hz)
F15	$R_1,R_2\uparrow$	14.36	125.89
F16	$R_1,R_2\downarrow$	2.43	316.23
F23	$R_a,R_f\uparrow$	0.30	146.43
F24	$R_a,R_f\downarrow$	17.64	184.78
F25	$R_a,C_1\uparrow$	0.17	135.94
F26	$R_a,C_1\downarrow$	17.62	251.19
F27	$R_a,C_2\uparrow$	2.98	135.94
F28	$R_a,C_2\downarrow$	17.06	251.19
F29	$R_f,C_1\uparrow$	2.31	116.32
F30	$R_f,C_1\downarrow$	17.18	292.86

TABLE VIIIV

FAULT DICTIONARY FOR TRIPLE FAULTS

Fault ID	Faulty Components	Peak Gain (dB)	Frequency at Peak Gain (Hz)
F35	$R_1,R_2,C_1\uparrow$	10.47	92.39
F36	$R_1,R_2,C_1\downarrow$	4.18	397.16
F37	$R_a,R_b,C_2\uparrow$	8.34	135.61
F42	$R_1,R_a,C_1\downarrow$	16.91	367.82
F43	$R_2,R_a,C_1\uparrow$	2.99	107.72
F44	$R_2,R_a,C_1\downarrow$	16.75	367.82
F47	$R_2,R_f,C_1\uparrow$	4.75	99.76
F48	$R_2,R_f,C_1\downarrow$	9.09	428.85

TABLE IX

FAULT DICTIONARY FOR OTHER MULTIPLE FAULTS

Fault ID	Faulty Components	Peak Gain (dB)	Frequency at Peak Gain (Hz)
F49	$R_1,R_2,R_a,R_f\uparrow$	1.75	107.72
F50	$R_1,R_2,R_a,R_f\downarrow$	17.31	397.16
F51	$R_1,R_2,R_a,C_1\uparrow$	2.06	99.76
F55	$R_2,R_b,C_1,C_2\uparrow$	17.03	99.76
F56	$R_2,R_b,C_1,C_2\downarrow$	-5.15	501.19
F57	$R_b,R_f,C_1,C_2\uparrow$	8.33	99.76
F58	$R_b,R_f,C_1,C_2\downarrow$	-3.69	584.34
F61	Fault Free	6.33	158.49

It may be noted from the above tables that for every faulty configuration, there exists a unique pair of parameters. This ensures that every fault in the dictionary is capable of being isolated without any ambiguity. This technique may even be extended to faults that are below 50%, i.e. 20%, 10% and even 5%. Tables X, XI and XII show a few selected NI ELVIS measurements taken for the above three deviations respectively. It may be noted that at least one of the two parameters is unique for every condition.

TABLE X

PARAMETER MEASREMENTS FOR 20% DEVIATIONS

Fault ID	Faulty Components	Peak Gain (dB)	Frequency at Peak Gain (Hz)
F2	$R_1\downarrow$	5.22	158.49
F15	$R_1,R_2\uparrow$	6.90	125.89
F16	$R_1,R_2\downarrow$	3.96	199.53
F35	$R_1,R_2,C_1\uparrow$	7.06	141.25
F36	$R_1,R_2,C_1\downarrow$	4.66	251.19
F39	$R_1,R_2,C_2\uparrow$	9.39	135.94

TABLE XI

PARAMETER MEASREMENTS FOR 10% DEVIATIONS

Fault ID	Faulty Components	Peak Gain (dB)	Frequency at Peak Gain (Hz)
F2	$R_1\downarrow$	5.21	158.49
F15	$R_1,R_2\uparrow$	6.03	158.49
F16	$R_1,R_2\downarrow$	4.41	158.49
F35	$R_1,R_2,C_1\uparrow$	5.78	158.49
F36	$R_1,R_2,C_1\downarrow$	6.03	199.53
F39	$R_1,R_2,C_2\uparrow$	6.98	158.49

TABLE XII

PARAMETER MEASREMENTS FOR 7% DEVIATIONS

Fault ID	Faulty Components	Peak Gain (dB)	Frequency at Peak Gain (Hz)
F1	$R_1\uparrow$	5.91	158.49
F2	$R_1\downarrow$	5.98	177.83
F3	$R_2\uparrow$	6.68	158.49
F4	$R_2\downarrow$	5.47	177.83
F5	$R_a\uparrow$	5.19	158.49
F6	$R_a\downarrow$	7.49	177.83

5. DIAGNOSIS METHODOLOGY

5.1 Comparison between theoretical and practical parameter measurements

Considerable differences arise between the parameter values estimated through theoretical and practical means. Comparison graphs may be drawn between the parameter values obtained in the theoretical and practical measurements to get an idea as to the extent to which non-ideal disturbances can affect the response of the circuit. Separate comparison graphs can be drawn for the two parameters. Fig. 5 shows the differences between the values of peak gain for single faults obtained in MATLAB and using NI ELVIS. It may be inferred from the graphs that the practical values curve more or less traces the precedent set by the theoretical values curve except at a few places. This is sufficient proof that the behaviour of the circuit is as required by design. Similar curves can be plotted for the other faults as well. In a similar fashion,

comparison graphs can also be drawn for the frequency parameter. Fig 6 shows the differences in frequencies between theoretical and practical observations for triple faults.

It can be clearly inferred from the comparison graphs that there is a marked difference, for some fault cases, between the theoretically calculated values and those measured in practice. Hence, it would not be advisable to solely depend upon the theoretically obtained parameter values while judging faults in a given circuit. Concessions must be made because of the deviations encountered in practical measurements of parameters. These deviations from the ideal are usually unpredictable in extent and may be caused due to a number of reasons such as saturation, tolerances of components, effects of wire parameters, stray capacitances and structural defects.

5.2 Oscillatory Conditions

For the given Sallen-Key circuit, certain components are chosen based on conditions that should be obeyed for an effective output from the op-amp.

For the Sallen-Key circuit,

$$1 + \frac{R_b}{R_a} < 3db \;\&\; R_f = R_1$$

are the conditions. If R_a gets reduced by 50%, then there occur oscillations in the gain values as shown in Fig. 7.

This behaviour can be explained on the basis of the Eigen values of the system. Table XIII shows the Eigen values for all the single faults. By using these values, we can determine the stability of the system for every fault type.

TABLE XIII

EIGEN VALUES FOR SINGLE FAULT CONDITIONS

Circuit Configuration	Eigen Values
Fault Free	1.0e+002 *(-4.5455 ± 8.3814i)
$R_2\uparrow$	1.0e+002 *(-3.0303 ± 7.1710i)
$R_a\uparrow$	1.0e+002 *(-6.3102 ± 7.1478i)
$R_f\uparrow$	1.0e+002 *(-6.2121 ± 6.0965i)
$R_2\downarrow$	1.0e+003 *(-1.0000 ± 1.0000i)
$\mathbf{R_a\downarrow}$	1.0e+002 *(**1.4545** ± 9.4230i)
$\mathbf{R_f\downarrow}$	1.0e+003 *(**0.0258** ± 1.1598i)
$C_1\downarrow$	1.0e+003 *(-0.6818 ± 1.1633i)

The real parts of the Eigen values should have negative value which shows the position to be on the left hand side of the S-plane. Then, the circuit is said to be stable. It may be noted from the above table that for the $R_a\downarrow$ and $R_f\downarrow$ conditions (in bold), the Eigen values have positive real parts (in bold), meaning that they are present in the RHS of the S-plane. This indicates its instability, which results in oscillations.

6. CONCLUSION

In this work, we have proposed a technique for the diagnosis of faults in analog circuits and illustrated the fault detection and isolation capabilities of the system through the example of the Sallen-Key band pass filter. Unique signatures were obtained for nearly all fault configurations of the circuit, which facilitated clear distinction between the various faults. The transition from the modeling environment, with all its ideal computations, to the real environment of the NI ELVIS shows the differences that can arise between the ideal and practical responses of a circuit for certain fault conditions. However, it is found that the response of the system is fairly well-matched between the theoretical and practical cases for most faulty configurations. Owing to this, the fault diagnosing capabilities of a system estimated through modeling and simulation can be safely transferred to the practical world.

REFERENCES:

[1] R. W. Liu, "Testing and Diagnosis of Analog and Systems", Van Nostrand, New York, NY, USA, 1991.

[2] R. W. Liu, "Selected Papers on Analog Fault Diagnosis, *IEEE Press, New York*, NY, USA,1987..

[3] J.W.Bandler and A. E. Salama, "Fault diagnosis of analog circuits", *Proceedings of the IEEE*, vol. 73, no. 8, 1985, pp. 1279–1325.

[4] Gertler,J.J., "Fault Detection and Diagnosis in Engineering Systems", *Marcel Dekker*, New York, 1998.

[5] Chen,J.,Patton,R.J., "Robust Model-Based Fault Diagnosis for Dynamic systems", *Kluwer Academic Publishers*, Masssachusetts, 1999.

[6] J. A. Starzy and J. W. Bandler, "Multiport approach to multiple fault location in analog circuits," *IEEE Trans. Circuits Syst.*, vol. 30, 1983, pp. 762–765.

[7] M. Tadeusiewic and M. Korzybski, "A method for fault diagnosis in linear electronic circuits",

Int. J. Circuits Theor. Applications, vol. 28, 2000, pp.254–262.

[8] G. Fedi, R. Giomi, A. Luchetta, S. Manetti, and M. C. Piccirilli, "On the application of symbolic techniques to the multiple fault location in low testability analog circuits," *IEEE Trans. Circuits Syst. II*, vol. 45, Oct. 1998, pp.1383–1388.

[9] R. Spina and S. Upadhyaya, "Linear circuit fault diagnosis using neuromorphic analyzers," *IEEE Trans. Circuits Syst. II*, vol. 44, March 1997, pp. 188–196.

[10] W. Hochwald and J. D. Bastian, "A dc approach for analog fault dictionary determination," *IEEE Trans. Circuits Syst. I*, vol. 26, May 1979, pp. 523–529.

[11] K. C. Varghese, J. H.Williams, and D. R. Towill, "Simplified ATPG and analog fault location via a clustering and separability technique," *IEEE Trans. Circuits Syst.*, vol. 26, May 1979, pp. 496–505.

[12] A. Mckeon and A. Wakeling, "Fault diagnosis in analogue circuit using AI technique," in *IEEE Int. Test Conf*., 1989, pp. 118–123.

[13] Bharat Ram R.., Prasanna Moorthy V., Devarajan N., "Fuzzy based time domain analysis approach for fault diagnosis of analog electronic circuits", *International Conference on Control, Automation, Communication and Energy Conservation*,2009.

[14] A. Balivada, J. Chen, and J. Abraham, "Analog testing with time reponse parameters", *Design and test of computers, IEEE*, Volume 13, Issue 2, Summer 1996.

[15] Somayajula, S.S. Sanchez-Sinencio, E. Pineda de Gyvez.J, "Analog fault diagnosis: a fault clustering approach", *Proceedings of European Test Conference*, Third, 1993.

[16] Vermeiren, W. Straube, B. Hohn, C., "On the application of fault detection observers to analog circuit testing", *Proceedings of European Test Conference,* Third, 1993.

[17] McKeon, A., Wakeling, A., "Fault diagnosis in analogue circuits using AI techniques", *Test Conference, Proceedings. International Meeting the Tests of Time,* 1989.

[18] Sergey G. Mosin, "Neural Network-Based Technique for Detecting Catastrophic and Parametric Faults in Analog Circuits", ICSEng, pp.224-229, *18th International Conference on Systems Engineering*, 2005.

[19] F. Grasso, S. Manetti, M.C. Piccirilli, "An Approach to Analog Fault Diagnosis Using Genetic Algorithms", *MELECON 2004*, Dubrovnik, Croatia.

[20] Contu, S. Fanni, A. Marchesi, M. Montisci, A. Serri A, "Wavelet analysis for diagnostic problems", *8th Electrotechnical Conference Mediterranean,* MELECON 1996.

[21] V. C. Prasad and N. Sarat Chandra Babu, "Selection of Test Nodes for Analog Fault Diagnosis in Dictionary Approach", *IEEE Transactions on Instrumentation and Measurement*, Vol. 49, No. 6, December 2000.

[22] Grzechca D., Rutkowski J., "New concept to analog fault diagnosis by creating two fuzzy-neural dictionaries test", *Proceedings of the 12th IEEE Mediterranean Electrotechnical Conference*, MELECON '04.

AUTHOR PROFILES:

V.Prasanna Moorthy received the M.E., degree in Power Electronics and Drives from Anna University, Chennai in 2005.

He is currently, Assistant Professor in the Department of Electrical Engineering, Government College of Technology, Coimbatore. His research interests are Fault diagnosis of circuits, Special Machines and Power Electronics.

N.Devarajan received the M.E., and Ph.D., degrees in Electrical Engineering from Bharathiar University, Coimbatore in 1989 and 2000 respectively.

He is currently, Assistant Professor in the Department of Electrical Engineering, Government College of Technology, Coimbatore. His research interests include Control Systems, Fault diagnosis of circuits and Electrical Drives.

ALL IMAGES WHICH NEED TO BE PRINTED IN COLOR NEED TO BE PLACED SEPARATELY ON THE LAST PAGE AND REFERENCED IN TEXT ACCORDINGLY

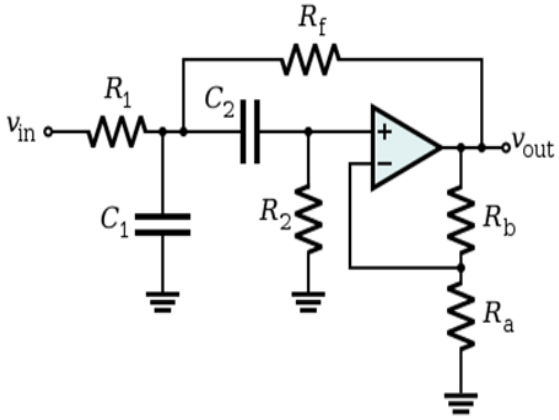

Figure 1. Sallen-Key band pass filter

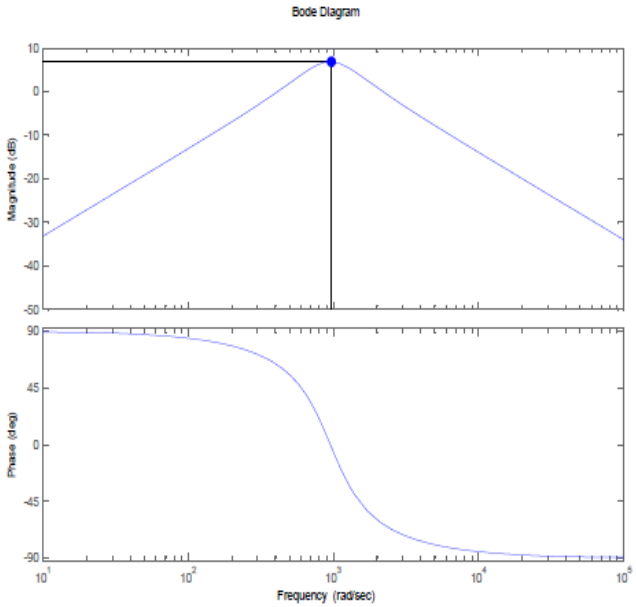

Figure 2. Bode plot for fault free condition

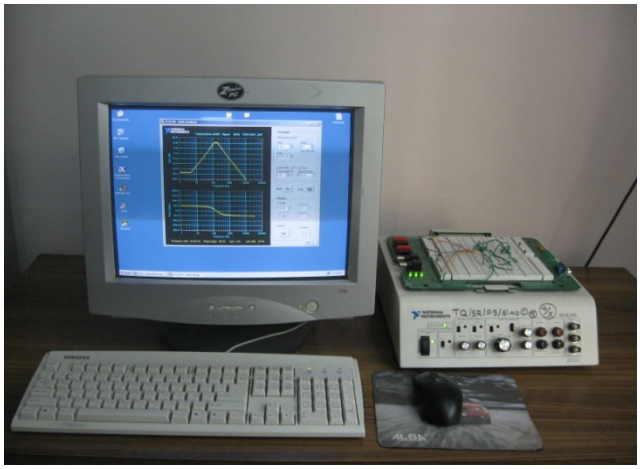

Figure 3. Experiment set up

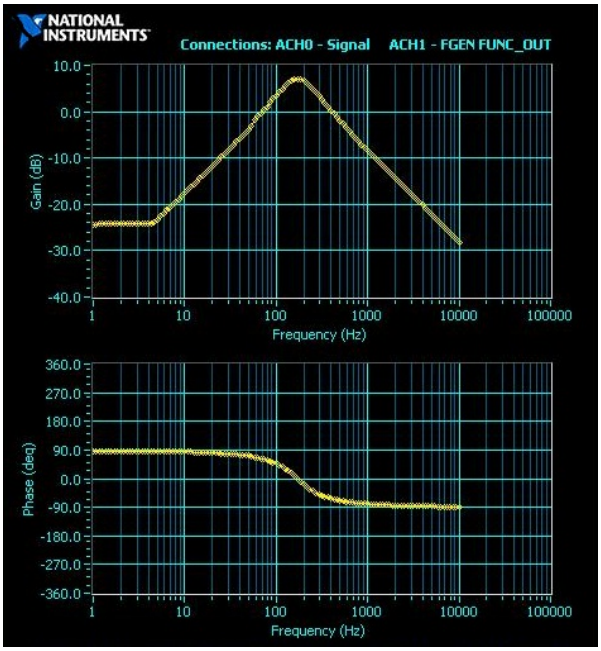

Figure 4. Bode plot for fault free condition

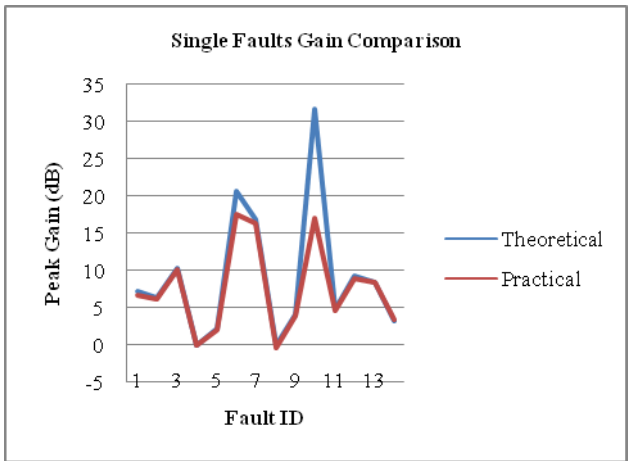

Figure 5. Comparison of Peak Gain values for single faults

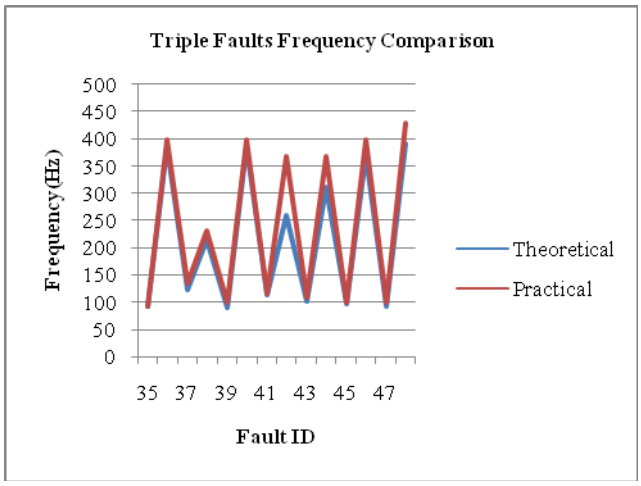

Figure 6. Frequency comparison graph for triple faults

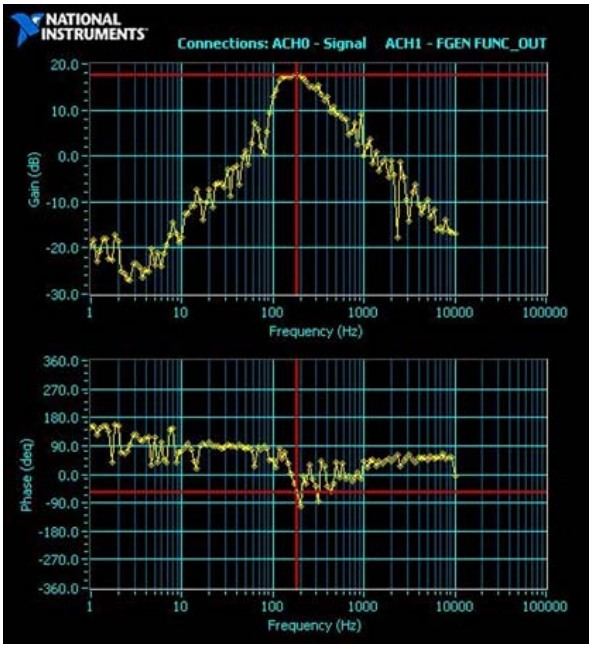

Figure 7. Oscillations in gain and phase